

Thermal Analysis Characterization of the Degradation of Biodegradable Starch Blends in Soil

A. Vallés Lluch,¹ A. Martínez Felipe,¹ A. Ribes Greus,¹ A. Cadenato,² X. Ramis,² J. M. Salla,² J. M. Morancho²

¹Department of Applied Thermodynamics, Escuela Técnica Superior de Ingenieros Industriales, Universidad Politécnica de Valencia, Carmino de Vera s/n, 46022 Valencia, Spain

²Laboratory of Thermodynamics, Escola Tècnica Superior d'Enginyeria Industrial, Universitat Politècnica de Catalunya, Avinguda Diagonal 647, 08028 Barcelona, Spain

Received 15 April 2004; accepted 11 October 2004

DOI 10.1002/app.21428

Published online in Wiley InterScience (www.interscience.wiley.com).

ABSTRACT: Dynamic mechanical thermal analysis, differential scanning calorimetry (DSC), and thermogravimetric analysis were used to monitor the degradation of biodegradable blends in soil from vegetal sources consisting of dispersed thermoplastic starch and cellulosic derivatives. First, the viscoelastic behavior of this blend was studied. A prominent relaxation process at about 90°C and an overlapped small relaxation in the vicinity of 160°C were identified and characterized. The specific parameters were evaluated as a function of the soil burial time. Interesting changes in the mechanical relaxation spectra were observed. The intensity of the prominent peak at 90°C tended to decrease with degradation as a result of the reduction in the number of amylose chains in the starch. Second, thermogravimetric thermograms provided a register of the moisture content in the samples and the starch chain removal due

to the degradation process. The nonisothermal kinetics of the decomposition processes were analyzed by means of Broido's integral method. The thermal stabilities of the non-degraded and degraded blends were estimated. The activation energies related to the correspondent reactions were calculated and evaluated as a function of the soil burial time. Furthermore, we used DSC as a complementary characterization technique to obtain information about the combined effect of moisture and the morphological changes that took place at molecular levels during the biodegradation process. © 2005 Wiley Periodicals, Inc. *J Appl Polym Sci* 96: 358–371, 2005

Key words: biodegradable; thermogravimetric analysis (TGA); mechanical properties; differential scanning calorimetry (DSC)

INTRODUCTION

Interest in degradable plastics has greatly grown during recent decades as a result of the increase in solid waste and the decrease in the capacity of rubbish dumps to store them. However, the goal for the future is still more ambitious. It is not enough to produce polymeric materials functional while in service and degradable after their use, but these materials must be produced from natural sources instead of petrochemical ones. The use of biotechnological polymeric materials obtained from renewable sources offers many environmental advantages compared with conventional polymers obtained from fossil resources.^{1,2}

Starch is an abundant natural polymer and is renewable, biodegradable and inexpensive. It consists of a glucose monomer joined by α -1,4 linkages, the so

called amylose, and a glucose monomer joined by α -1,4 linkages with branch points involving α -1,6 linkages, the so called amylopectin. Starch is the main polysaccharide in terms of vegetal energy storage, and it can be found in lots of sources, including corn, potato, rice, wheat, barley, oats, and tapioca. It possesses a low permeability, which is what makes it suitable for packing.

Starch can be blended with different polymers, such as cellulose derivatives, to satisfy specific market needs. Cellulose is also a linear polysaccharide with a high molecular weight, which provides plants rigidity due to its high modulus. Their chemical structures differ by the fact that in starch, the glucose rings are linked by carbons 1 and 4 by α rather than β linkages, apart from its branching.

In this study, the studied biopolymer was a blend obtained from vegetal sources consisting of thermoplastic starch in a dispersed form and cellulose derivatives,¹ referred to as Mater-Bi class Y (Novamont SpA, Novara, Italy). Due to its inherent characteristics, this material can act as a substitute for traditional plastics, such as polyethylene or polystyrene, in several applications (rigid and dimensionally stable

Correspondence to: A. R. Greus (aribes@ter.upv.es).

Contract grant sponsor: Ministerio de Ciencia y Tecnología of Spain; contract grant number: PPQ2001-2764-C03-01/02.

Contract grant sponsor: Instituto Tecnológico del Plástico.

TABLE I
Average Mechanical and Physical Characteristics of Mater-Bi Class Y

Property	Value range
Minimum processing temperature	140°C
Maximum processing temperature	210°C
Density	1.34 g/cm ³
Tensile stress at break	26 MPa
Elongation at break	27%

molded injected articles, food packing, etc.). Furthermore, it is capable of degradation at the end of its useful life, which closes the carbon cycle. Mater-Bi can be processed as films in coverts for agriculture purposes because it degrades into nondangerous products in contact with the microorganisms in the soil.³

Thermal analysis techniques provide a powerful research tool for obtaining qualitative and quantitative information about the effects of biodegradation on the structure and other important properties of the degraded material.⁴⁻⁶ Among thermoanalytical techniques, dynamic mechanical thermal analysis (DMTA), thermogravimetric analysis (TGA), and differential scanning calorimetry (DSC) have been used to investigate the degradation of Mater-Bi. For this purpose, several samples were submitted to an accelerated soil burial test for different time periods up to 212 days. Both nondegraded and degraded samples

were analyzed. These studies provided information about the chemical modifications and physical transitions that took place in the blend due to the degradation process.

EXPERIMENTAL

Materials

Granular Mater-Bi class Y, consisting of thermoplastic starch in a dispersed form and cellulose derivatives, was supplied by Novamont SpA. This material is a biodegradable and compostable biopolymer made from raw materials of natural origin, and its moldability is very close to that of polystyrene.¹ Some of its average physical and mechanical properties are summarized in Table I.

Samples were prepared by compression molding in a Collin PCS-GA type PRESSE x800 (Wellingborough, UK) as sheets 145 × 145 × 2 mm in size in the temperature range 195 to 60°C and with silicone oil as a mold-release agent. These sheets were then cut out as bars 145 × 10 × 2 mm in size.

Accelerated soil burial test

The samples were subjected to an accelerated degradation test, following the DIN 53739 International Norm.⁷ Samples were buried in biologically active soil contained in rectangular plastic boxes, which were

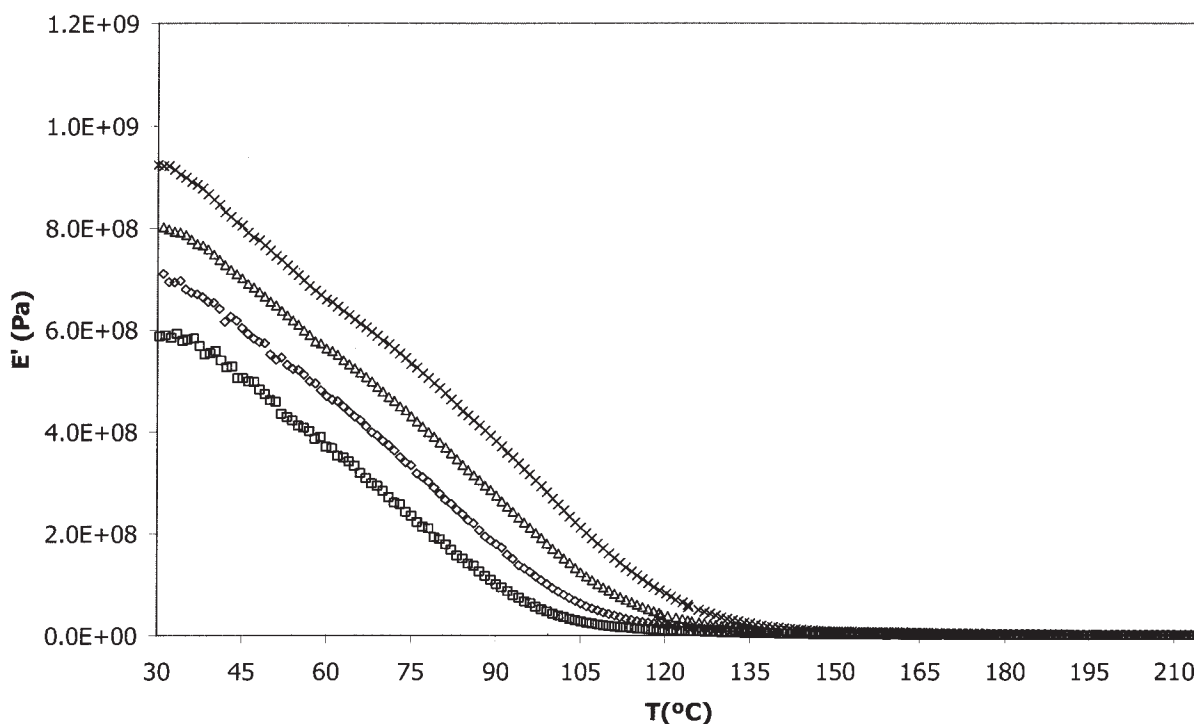


Figure 1 Mechanical spectra in terms of E' as a function of temperature for the nondegraded sample at frequencies of (□) 0.05, (◇) 0.5, (▲) 5, and (×) 50 Hz.

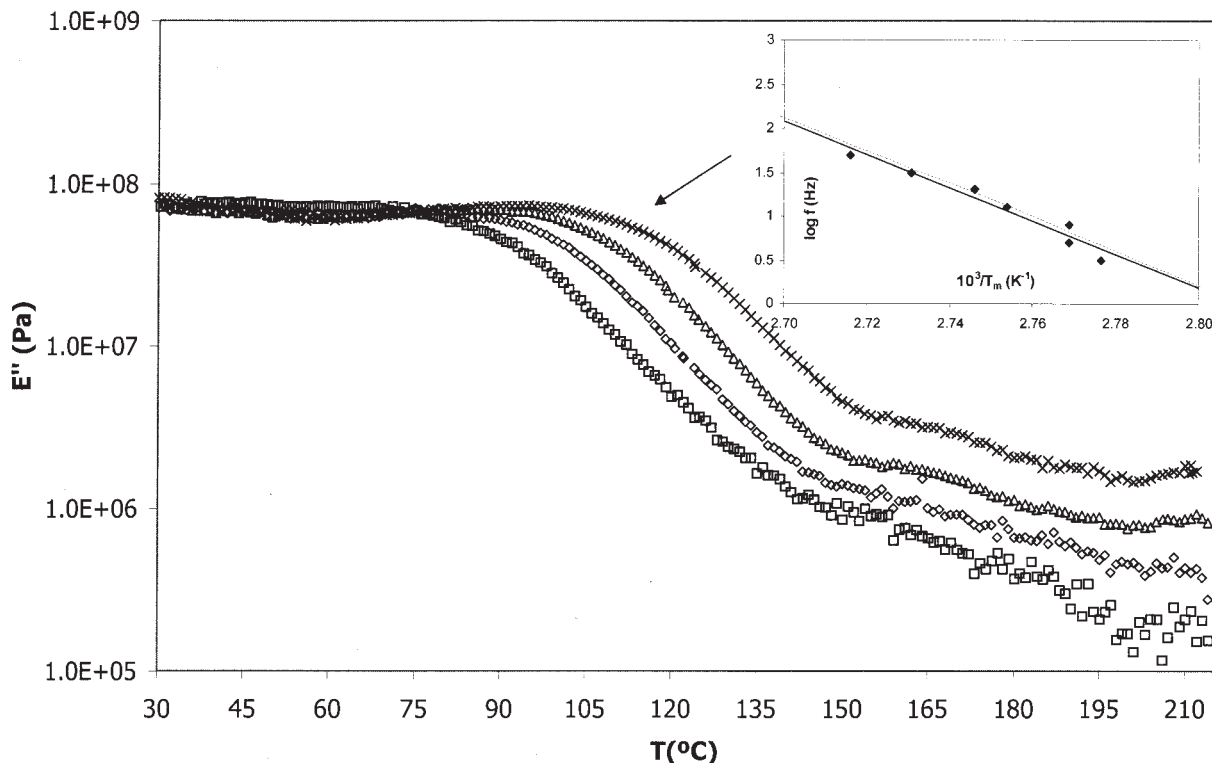


Figure 2 Mechanical spectra in terms of E'' as a function of temperature for the nondegraded sample at frequencies of (\square) 0.05, (\diamond) 0.5, (\blacktriangle) 5, and (\times) 50 Hz.

kept opened to ensure an adequate oxygen supply. Previously, the boxes were lined on the inside with a stainless iron cloth to ensure good air circulation.⁸

The soil was a 50/50 wt % mixture of a soil extract picked up from a culture field and a soil usually used in greenhouses for growing pines. Before its use, the soil was passed through a sieve to remove stones, macro-organisms, and any other residues.

The boxes were kept in Heraeus B12 culture ovens (Hanau, Germany) at a constant temperature of $28 \pm 0.5^\circ\text{C}$, and we periodically controlled the pH and the water content of the soil. pH values were measured from a soil extract dissolved in distilled water in a 1:20 proportion. The pH was maintained at approximately 7, and the humidity was maintained at 60% of the soil maximum-water-retention capacity.

The samples were subjected to different exposure times in the soil of up to 212 days. When the samples were removed, they were carefully washed with soap dissolution and dried afterwards to stop the biodegradation process. Some of the samples were kept nondegraded for use as references.

DMTA

The viscoelastic properties were determined by means of a Mark IV dynamic mechanical thermal analyzer from Rheometric Scientific (Piscataway, NJ). Deforma-

tion was applied in the cantilever double-clamping bending mode. The storage modulus (E'), loss modulus (E''), and damping or loss tangent ($\tan \delta$) were measured from 30 to 215°C in isothermal steps, each 1°C, in a frequency range from 0.05 to 50 Hz, with 5 points taken per decade in the logarithmic scale.

TGA

TGAs were carried out in a Mettler TGA/SDTA 851 analyzer (Columbus, OH). We performed measurements following a dynamic program from 25 to 700°C at a heating rate of 20°C/min under an argon atmosphere. Sample masses were between 7 and 10 mg.

DSC

Calorimetric experiments were performed with a Mettler Toledo DSC-30. The samples (9–11 mg) were weighed out in a standard aluminum pan. The sealed pans were scanned at a heating rate of 10°C/min from room temperature to 220°C under a nitrogen atmosphere (first scan). After the temperature was held at 220°C for a minute, the samples were cooled to room temperature and then rescanned to 220°C at the same heating rate (second scan).

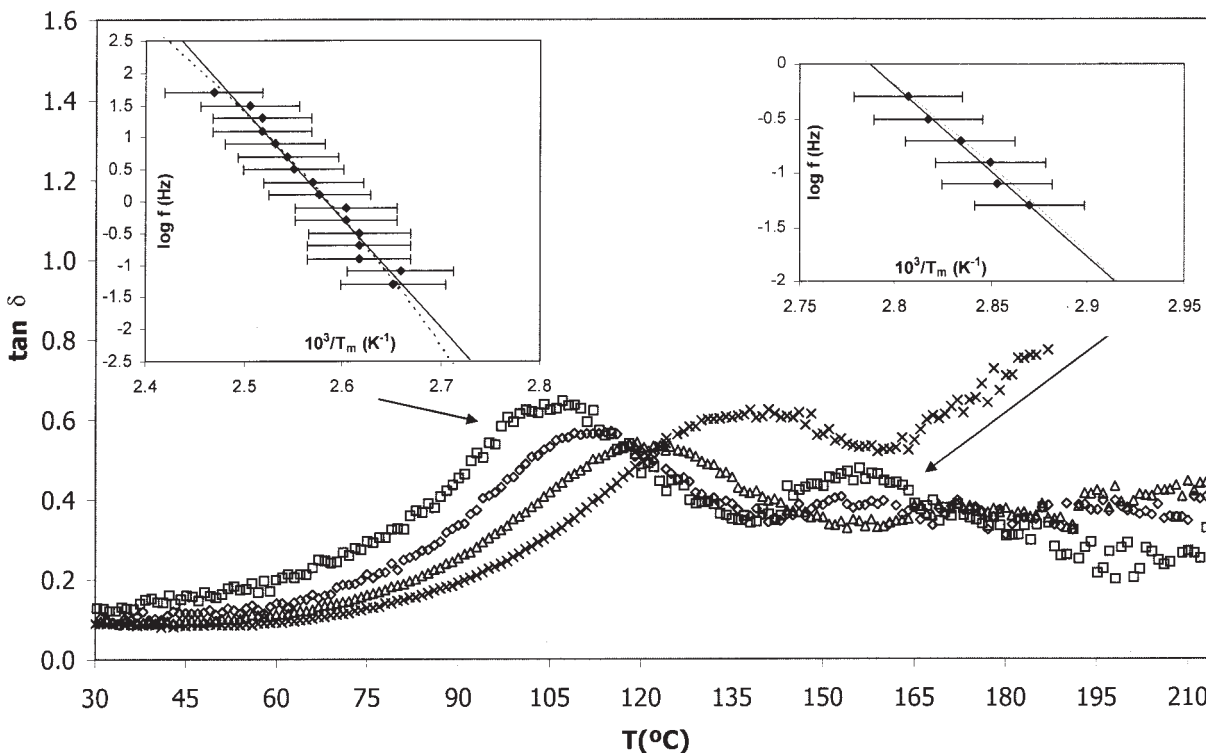


Figure 3 Mechanical spectra in terms of $\tan \delta$ as a function of temperature for the nondegraded sample at frequencies of (\square) 0.05, (\diamond) 0.5, (\blacktriangle) 5, and (\times) 50 Hz.

RESULTS AND DISCUSSION

The viscoelastic properties of the Mater-Bi blend before degradation were evaluated from its mechanical spectrum. The curves were plotted in terms of E' , E'' , and $\tan \delta$ as a function of the temperature.

TABLE II
Mechanical Characterization for the Nondegraded and Degraded Samples

Nondegraded samples		
	Low temperatures	High temperatures
m (K)	1540	1425
α_f ($10^{-3}/\text{K}^{-1}$)	0.65	0.70
E_a (kJ/mol)	318.15	300.93
Degraded samples		
Exposure time (days)	E_a (kJ/mol; low temperatures)	
0	318.15	
7	365.58	
14	386.01	
21	418.49	
28	389.69	
35	430.77	
42	339.80	
49	317.44	
59	330.71	

Figure 1 shows the frequency dependence of E' in the temperature range from 25 to 215°C for the nondegraded blend. It displayed a strong decrease as the temperature increased from the beginning of the measurement.

The spectra in terms of E'' are plotted in Figure 2. The E'' curves showed an intense main peak around 90°C (at a frequency of 1 Hz) for the nondegraded sample. A slight secondary peak was observed if a logarithmic scale axis was used.

Figure 3 presents $\tan \delta$ as a frequency function in the same temperature range. The two relaxation processes were well observed: the prominent peak with the maximum appeared at approximately 105°C (at a frequency of 1 Hz) and the secondary peak appeared at 165°C (at the same frequency).

According to the literature,⁸⁻¹⁰ only two broad peaks have been described from pure cellulose, one at -60°C, which is assigned to movements of OH primary groups in the amorphous regions of cellulose, and another at 10°C, which is ascribed to the moisture absorbed by the cellulose chains. Only cellulose derivatives (i.e., cellulose acetates) display a peak around 200°C. Because the measurements in this study were performed from 25°C, the entire complex relaxation zone observed in Figures 2 and 3 was supposed to be associated to the starch, and the peak appearing above

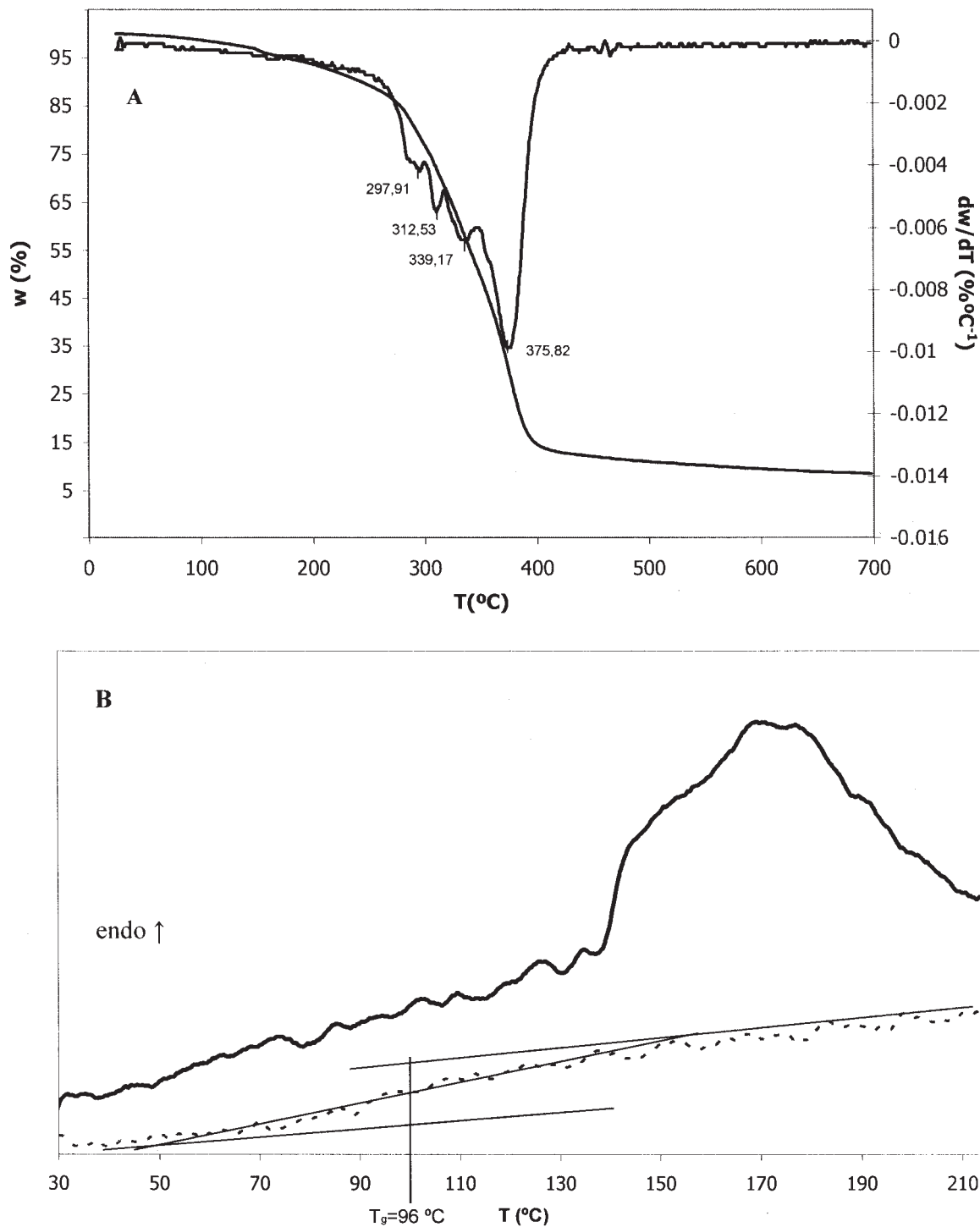


Figure 4 (A) TG and DTG curves and (B) DSC TGs for the first and second scans for the nondegraded sample.

200°C was related to the synthetic component of the cellulose.

To better understand the molecular origin of the principal (observed in E'' and $\tan \delta$) and the secondary (observed in $\tan \delta$) relaxation processes observed in the Mater-Bi blend, the temperatures of the maxima were obtained for each frequency (f), and the relaxation maps were plotted in Figures 2 and 3 with

continuous lines. If the origin of these relaxations rested on intramolecular movements, the temperature dependence of the relaxation times followed an Arrhenius dependence:

$$\log f = \log f_0 - \frac{E_a}{RT_m}$$

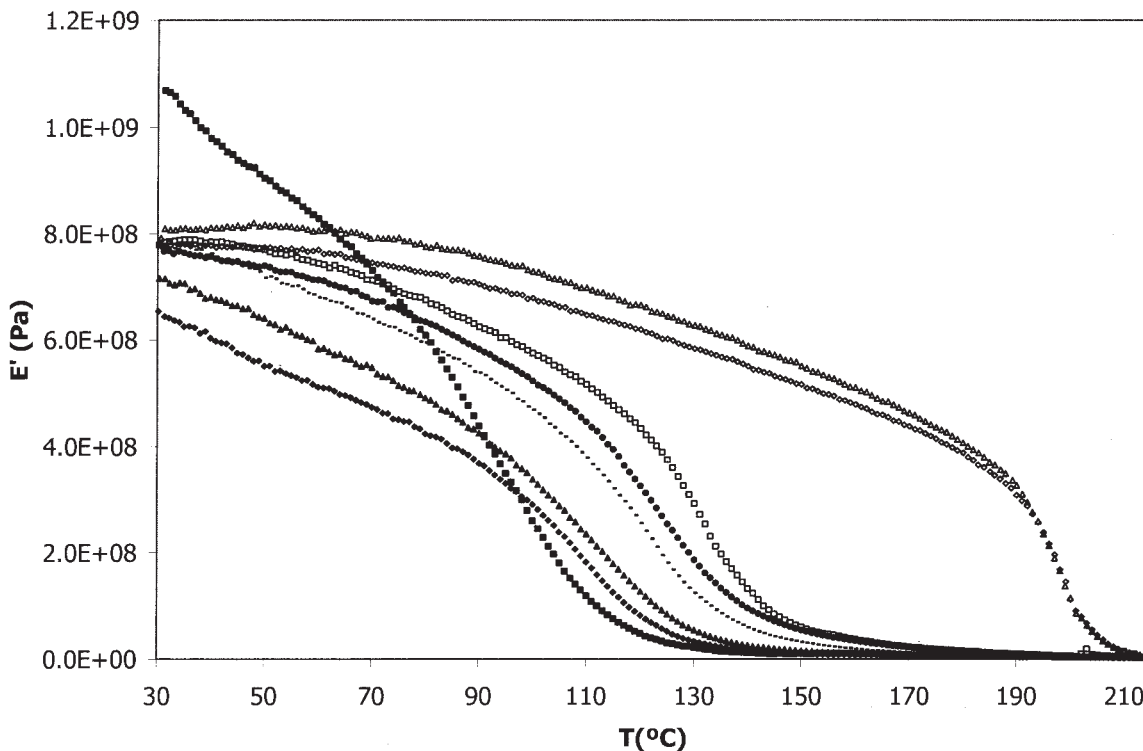


Figure 5 Mechanical spectra in terms of E' as a function of temperature for the samples degraded at 5 Hz for (■) 0, (◆) 7, (▲) 14, (-) 28, (●) 42, (□) 59, (◇) 145, (▲) 170 days.

where f_0 is a preexponential factor, R is the gas constant, and T_m is the peak temperature in the E'' or $\tan \delta$ curve. Linear regression of the data gave the apparent activation energies (E_a 's). The results obtained for both relaxations from $\tan \delta$ curves are summarized in Table II.

The values obtained were high enough to rule out the hypothesis of an intramolecular process. The good accuracy of the calculated regression may have been caused by the narrow frequency range used in the experiments. Thus, these results suggest that both processes could have involved cooperative intermolecular motions related to the glass-transition relaxation. If this hypothesis was assumed, the relationship between the relaxation times and the temperatures should have been adjusted for each sample to the Vogel–Fulcher–Tamman–Hesse (VFTH) equation:¹¹

$$\ln f = A - \frac{m}{T_m - T_\infty}$$

where the parameters A , m , and T_∞ (the temperature at which the free volume would be equal to zero) can be obtained for each sample. The m parameter is related to the thermal dilation coefficient (α_f) by

$$m = B \frac{T_g - T_\infty}{\phi_g} = \frac{B}{\alpha_f}$$

where B is a constant whose value is close to unity and ϕ_g is the free volume fraction in the sample. Figures 2 and 3 display the fittings. The dotted line corresponds to a nonlinear fitting according to the VFTH equation. α_f calculated from the main relaxation was $0.65 \cdot 10^{-3} \text{ K}^{-1}$, and α_f from the secondary relaxation was $0.70 \cdot 10^{-3} \text{ K}^{-1}$ from the $\tan \delta$ curves.

De Graaf et al.¹² suggested that the glass-transition temperature (T_g) of a starch material can range from 75 to 160°C as a function of the amylose/amylopectin ratio. Products containing a higher amount of amylopectin have higher T_g 's than materials with lower amylopectin contents. The lower molecular weight in the amylose and its lack of branchings allow the molecular chains to move more easily.

Avérous et al.¹³ reported a shift in T_g toward higher temperatures when a thermoplastic starch was reinforced with cellulose fibers. Thus, the emergence of cellulose–starch interactions would result in a reduction of the molecular motions of the starch chains.

The mechanical results suggest that the Mater-Bi blend formed an unhomogeneous material and that cooperative molecular movements of the chains in almost two different zones were produced.

TGA and DSC thermograms (TGs) were performed for the nondegraded Mater-Bi. The TG curve (TG) and its derivative plot (DTG) are traced in Figure 4(A). The DTG curve showed a complex decomposition step

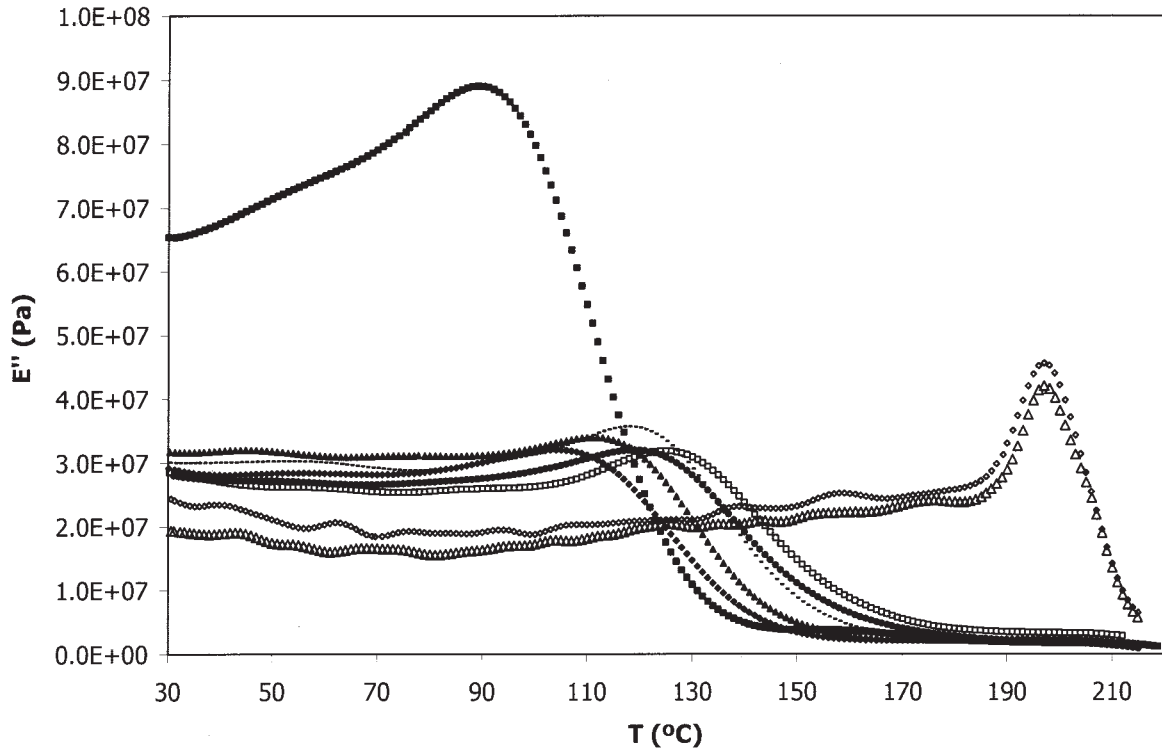


Figure 6 Mechanical spectra in terms of E'' as a function of temperature for the samples degraded at 5 Hz for (ν) 0, (\blacklozenge) 7, (\blacktriangle) 14, (-) 28, (\bullet) 42, (\square) 59, (\diamond) 145, (\blacktriangle) 170 days.

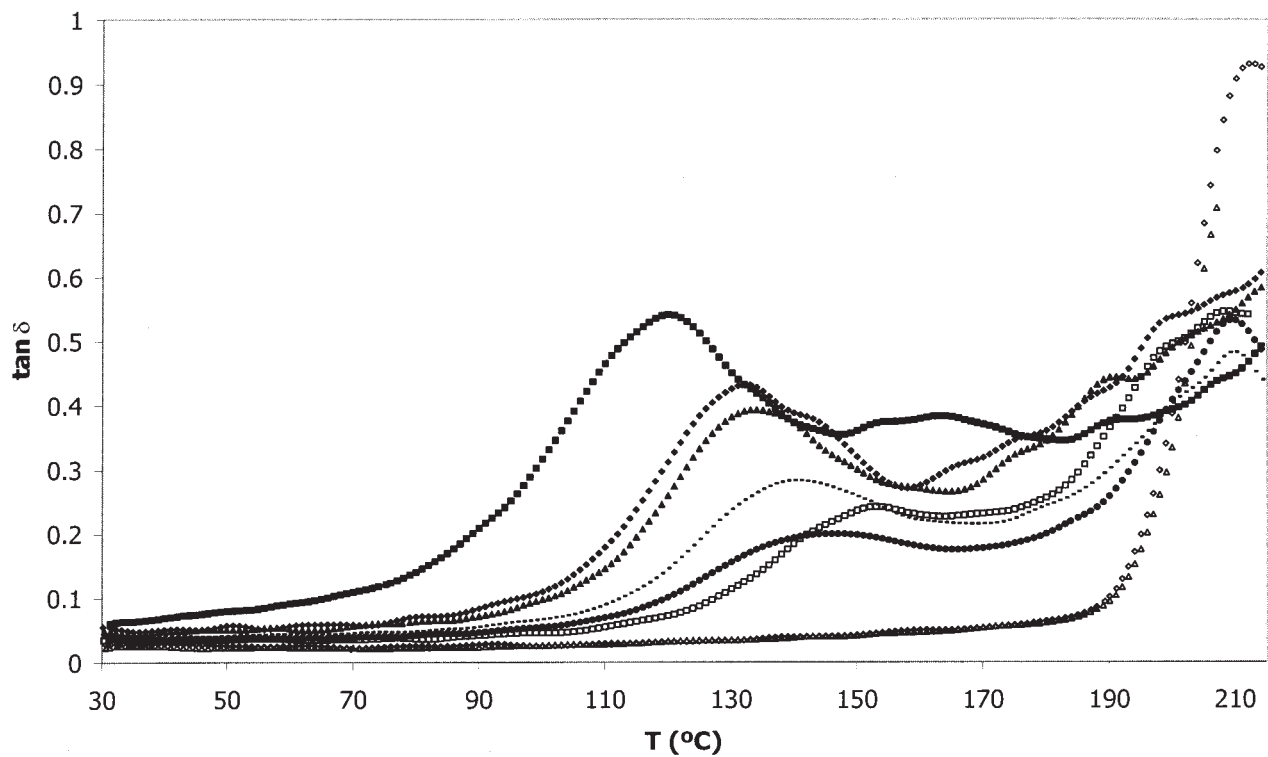


Figure 7 Mechanical spectra in terms of $\tan \delta$ as a function of temperature for the samples degraded at 5 Hz for (ν) 0, (\blacklozenge) 7, (\blacktriangle) 14, (-) 28, (\bullet) 42, (\square) 59, (\diamond) 145, (\blacktriangle) 170 days.

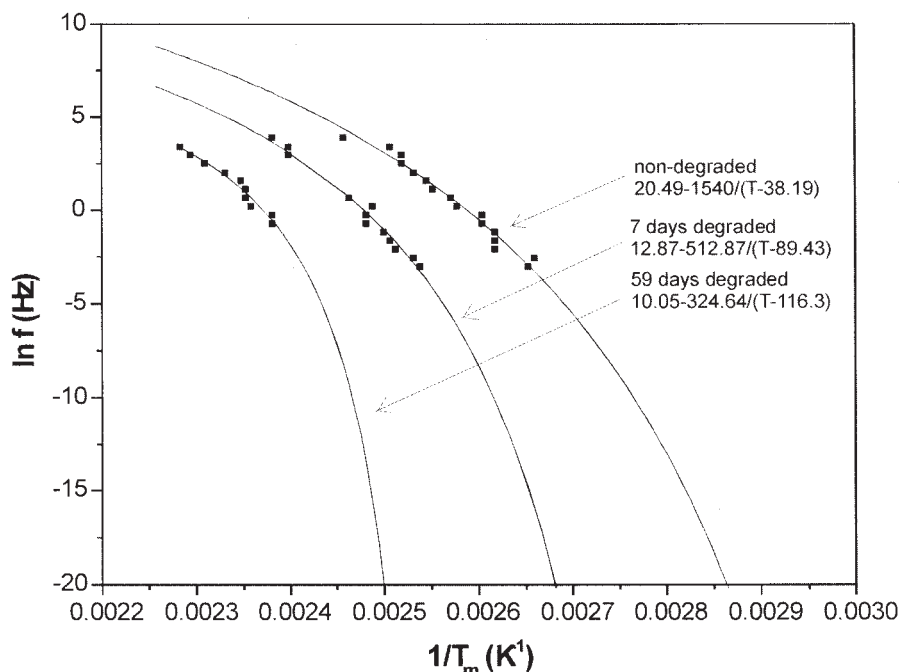


Figure 8 Fitting to the VFTH equation for the samples degraded for 0, 7, 21, and 59 days.

between 280 and 380°C and four peaks with maxima at 297, 312, 339, and 370°C.

The first three processes were related to the different decomposition rates of amylose and amylopectin chains and to the network structure of the cellulose.^{14,15} The amylose chains were the first decomposed component due to their linear structure. On the other hand, the mass loss at 370°C was attributed to the complete thermodecomposition of the synthetic compounds of cellulose. A loss of mass about 100°C was not observed. The absorbed water and, thus, the moisture content of the Mater-Bi blend were very low during the storage conditions.

Figure 4(B) displays the calorimetric TG of the non-degraded Mater-Bi blend. A broad endothermic transition was observed in the first scan in the temperature range from 140 to 210°C. Generally, T_g is computed as

the midpoint of the heat capacity increase, but it was difficult from these results to determine it because the small area corresponding to the endothermic peak overlapped the heat capacity increase. The shape of this broad peak denoted the heterogeneous morphology of the crystalline structures in the Mater-Bi blend. The endothermic peak did not appear in the second scan.

It was difficult to interpret the origin of this endothermic peak because there were many overlapped processes. A similar broad peak was also found by other authors around the same temperatures.¹⁶ They assigned it to the gelatinization of the material and found out that the enthalpy of this transition was strongly dependent on the moisture content.

Other authors¹⁷ have reported a broad endothermic peak from 163 to 230°C in dry starch. This peak was

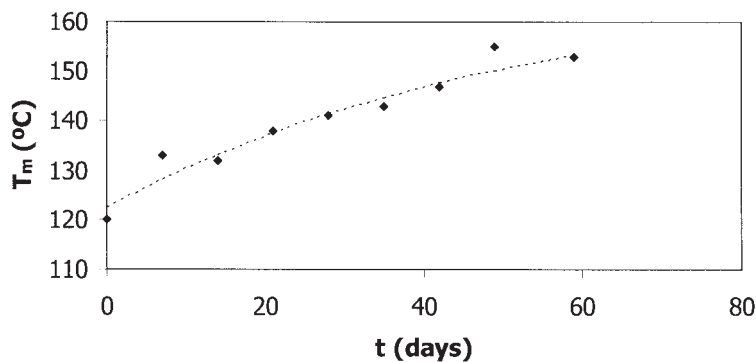


Figure 9 T_m corresponding to the glass transition at 5 Hz as a function of degradation time.

attributed to both melting and recrystallization by different ways of the amylose and amylopectin components and a volume relaxation process. Because the moisture content of the Mater-Bi blend was very low, as TGA results indicated, the endothermic peak could only have been related to the aforementioned processes.

It is believed that starch forms a layered structure, which consists of alternating crystalline regions and an amorphous background layer. Different types of morphological forms have been reported by other authors¹⁸ to describe the crystalline zone. One type is a more dense crystal packed in a monoclinic unit cell. In other types, double helices have been observed, which were interpenetrated by water channels, resulting in hexagonal unit cells. Thus, the crystalline parts were organized as highly crystalline lamellae intermitted by less perfect crystalline regions. The amorphous layers consisted of more disordered amylose and amylopectin chains, and the glass transition of this layer was observed.

On the other hand, when starch blends are stored, some starch chains can recrystallize by two different methods. The recrystallization process of amylose chains is an irreversible and very fast process. Amylopectin recrystallization is, by contrast, reversible and slower. A volume relaxation in the amorphous zone has also been described.¹² Hence, the broad endothermic peak obtained was the result of the total heat effects corresponding to the addition of all of the contributions.

The second scan was considered to better determine T_g . In this case, all of the thermal history of the sample was erased, and a slight glass transition was observed in the vicinity of 100°C as an inflexion point in the heat flow curve.

Effect of soil burial on the Mater-Bi blend

To analyze the changes produced on the Mater-Bi blends due to the degradation process, mechanical spectra were obtained for each one of the samples subjected to the soil burial test.

As examples, Figures 5, 6, and 7 display the mechanical spectra at a frequency of 5 Hz for some of the Mater-Bi samples that were degraded for different times in terms of E' , E'' and $\tan \delta$, respectively. Interesting effects of the degradation on the mechanical behavior of the Mater-Bi blends were quite visible.

As shown in Figure 5, E' decreased, the shape of the peak smoothened and widened, and the temperature of the start of the drop shifted to higher temperatures as degradation took place.

Figure 6 displays the curves in terms of E'' . The strong peak around 90°C for the nondegraded sample diminished and shifted toward higher temperatures as degradation occurred.

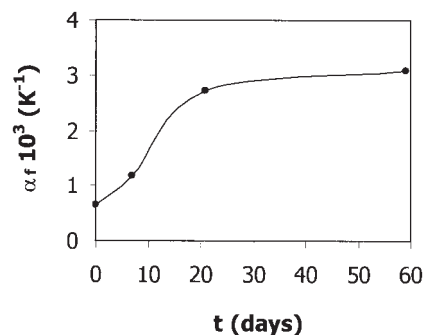


Figure 10 Evolution of α_f with degradation time.

The spectra in terms of $\tan \delta$ are plotted in Figure 7. As shown in these curves, the main peak shifted to higher temperatures, whereas its intensity decreased. A complex relaxation zone was formed as the time of the exposition in the soil increased. However, this drop in the intensity was progressive until total disappearance at 59 days. This result may have indicated a removal of some of the starch chains due to the degradation process.

If we assumed that this relaxation was related to the glass transition, the temperature dependence of the relaxation time would once again fit a VFTH equation. $\tan \delta$ curves were used for this purpose. Figure 8 shows as an example of the fitting to this equation for some of the samples degraded for different times. Only the results from samples degraded up to 59 days were adjusted because no relaxations were further observed.

Figure 9 shows the evolution of T_m with degradation time. This temperature increased gradually. This result was in agreement with the results of De Graaf et al.¹² T_g in the starch is related to the amylose and amylopectin ratio. If the temperature increases due to the degradation process, this is understood as a removal of the amylose chains.

Figure 10 displays the evolution of α_f with degradation time. α_f showed an initial increase, reaching a plateau at 20 days in the soil. This increase was explained by the fact that the disordered chains in the amorphous zone were broken because of the degradation process. Thus, a change in the intermolecular interactions of the chains that formed this zone could take place, and consequently, the free volume could increase.

In addition, TGAs were carried out to further investigate the changes in the chemical structure occurring during the biodegradation process. The resulting TG curves and their DTG plots are shown in Figure 11 for some of the degraded samples.

The main differences with respect to the nondegraded sample were

- The secondary thermal decomposition steps, which were related to the different decomposition

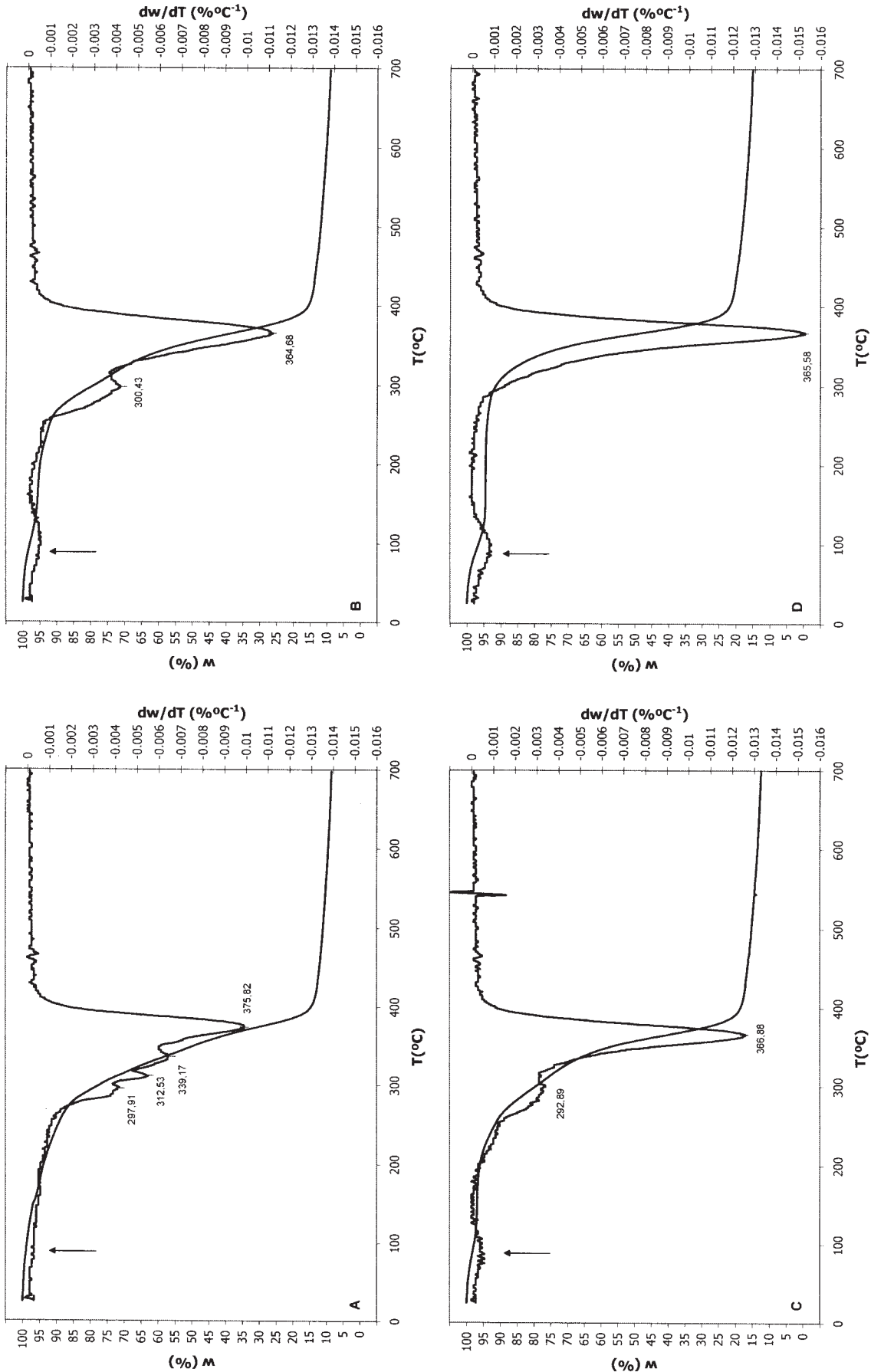


Figure 11 TG and DTG curves for the samples degraded for (A) 7, (B) 21, (C) 59, and (D) 87 days.

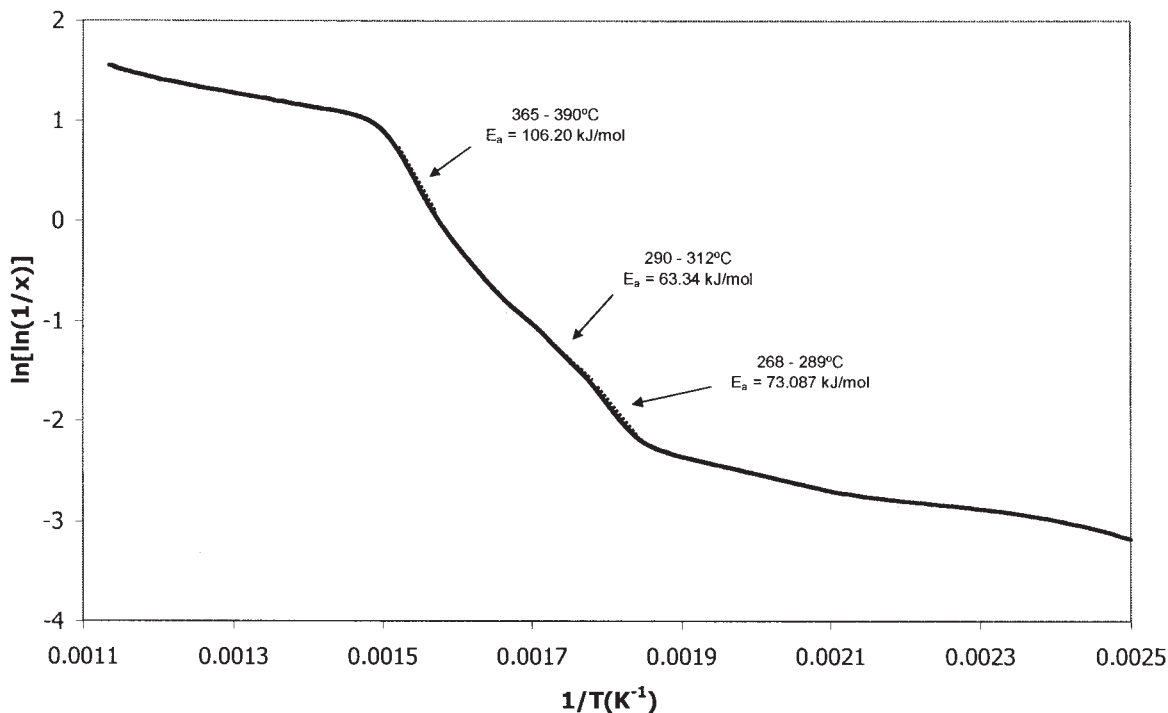


Figure 12 Fitting to the Broido equation for the sample degraded for 7 days.

rates of amylose and amylopectin and cellulose, tended to decrease and finally disappear after 87 days of degradation.

- The principal thermal decomposition process, which could be related to the derivative cellulose component, remained apparently unaltered.
- A slight peak at low temperatures, around 100°C, corresponding to the mass loss of the absorbed water, was observed. During exposition in soil, the blends increased their moisture content.

Changes in the thermal stability and the kinetic parameters that characterized the decomposition process provided information about the breakings of chains during the exposition time in soil. To determine the kinetic parameters, the different decomposition processes were fit to the Broido equation,¹⁹ from which slope the E_a could be calculated:

$$\ln \left[\ln \left(\frac{1}{x} \right) \right] = \frac{-E_a}{RT} + \text{Constant}$$

where T is the absolute temperature and x is the residual fraction defined as

$$x = \frac{\omega - \omega_\infty}{\omega_0 - \omega_\infty}$$

where ω_0 , ω , and ω_∞ are the sample weights initially, at time t , and at an infinite time, respectively.

Figure 12 displays, as an example, the fitting for a sample degraded in soil for 7 days. Three overlapped thermal decomposition processes were observed. The shape of the curves changed with time of degradation in the soil. The calculated E_a values are summarized in Table III for all of the samples.

These results suggest that at least three different types of chains, which behaved differently during the degradation process, could be distinguished. The thermal decomposition process appearing at the lowest temperature was associated with the shortest and linear chains of the amylose that suffered a fast decrease in their E_a values. The following process in the temperature axes were related to the thermal decomposition of amylopectin and pure cellulose, and their E_a values decreased more slightly. Although all of these samples were removed after 87 days, these results indicate that starch was progressively removed by the degradation in soil process.

The third decomposition process, appearing at the highest temperatures, was due to the backbone chains of the synthetic cellulose derivatives. This decomposition peak remained apparently unaltered or slightly shifted to lower temperatures with time in the soil. These thermogravimetric results were consistent with the mechanical results reported previously.

The increase in the moisture content produced a plasticizing effect. Plasticizers act by spacing out the molecules and reducing the interactions. Thus, cohesive forces decrease drastically, the polymer expands,

TABLE III
 E_a Values Calculated with the Broido Integral Method

Degradation time (days)	Temperature range (°C)	E_a (kJ/mol)	Temperature range (°C)	E_a (kJ/mol)	Temperature range (°C)	E_a (kJ/mol)
0			280–355	60.470	365–390	110.94
7	268–289	73.087	290–312	63.345	365–390	106.20
21	265–286	62.946	283–302	64.078	360–390	109.40
35	268–286	57.062	286–315	45.315	354–386	130.99
49	268–286	67.617	286–305	51.676	354–386	134.85
59	256–286	55.940	286–308	50.802	354–380	123.79
87	265–292	15.329	296–312	55.244	354–386	153.86
108	265–292	—	296–312	—	342–379	100.07
145	265–292	—	296–312	—	342–379	90.74
170	265–292	—	296–312	—	342–379	99.51

and the free volume increases. Nevertheless, it is well established that in an amorphous and homogeneous polymer, the plasticizer effect should lower T_g and make the starch more rubber-like.

However, from the mechanical experimental results, an increase in the temperature of the maximum damping module, related to T_g was observed. These results could be explained if we assumed that the starch was not a homogeneous material, and different processes (hydration, swelling, amylose leaching, gelatinization, etc.) could have occurred when water was absorbed from the soil. In addition, the removal of amylose chain increased the amylopectin/amylose ratio, and consequently, T_g should have also increased. This second effect was probably more important than the plasticizing effect and, thus, overlapped it.

To analyze the morphology of the samples and its evolution during the degradation, calorimetric scans were carried out for the samples degraded for different periods of time. Second scans were also performed to better determine the T_g values of the samples. The calorimetric TGs by the first and second scan are shown in Figures 13 and 14, respectively. For the nondegraded samples, the first scan showed a broad endothermic peak that did not appear in the second scan. Many interesting changes seemed to have taken place during the storage of the samples in soil at 28°C. It was very difficult to interpret any of the enthalpic processes because all of the contributions appeared to be overlapped. DSC curves reflected mainly the different losses of molecular order, gelatinization, and enthalpic changes related to the structural relaxations. All of them, however, seemed to be reversible and slow processes from the fact that they were not observed during the second scan.

The endothermic peak progressively narrowed, and its intensity increased with degradation time. If the width of the endothermic peak is understood as an estimation of the heterogeneity of the crystalline structures, these results suggest that only the most perfect crystalline regions did not suffer the attack

of microorganisms during the soil burial test. Because this peak was not removed after 87 days, it may have not only been related to the starch but

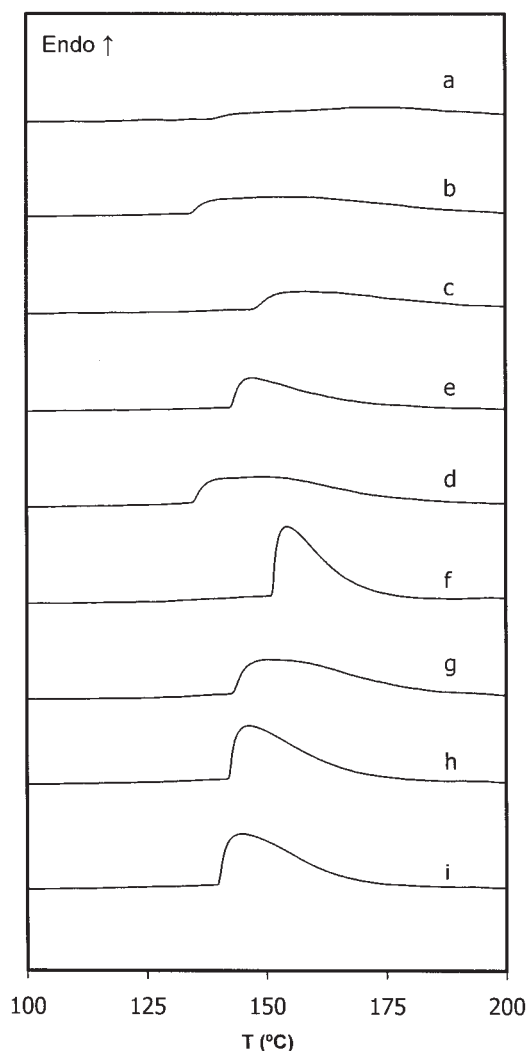


Figure 13 DSC TGs by the first scan for the samples degraded for (a) 0, (b) 7, (c) 21, (d) 42, (e) 87, (f) 108, (g) 145, (h) 170, and (i) 212 days.

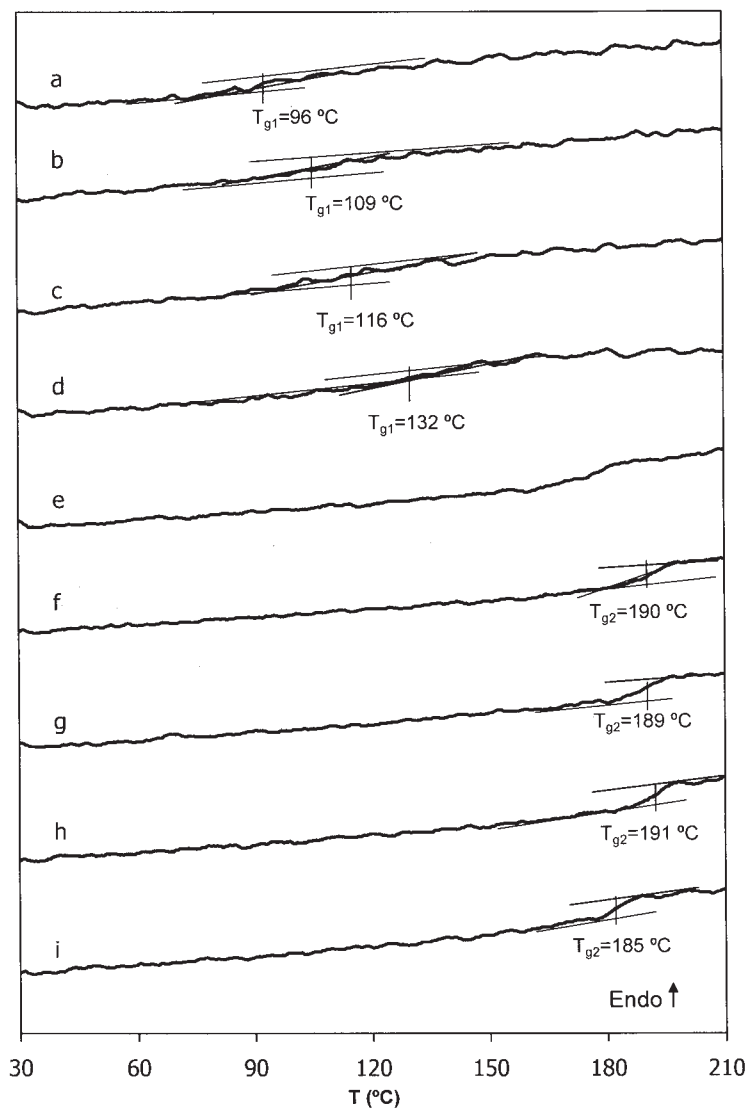


Figure 14 DSC TGs by the second scan for the samples degraded for (a) 0, (b) 7, (c) 21, (d) 42, (e) 87, (f) 108, (g) 145, (h) 170, and (i) 212 days.

may also have been related to the synthetic derivatives of cellulose.

A slight glass transition was observed in the vicinity of 100–130°C as an inflexion point in the heat flow curves in the second scan but only for samples degraded for times up to 87 days. This confirmed the removal of the starch by degradation in soil.

CONCLUSIONS

Different thermal analysis techniques, DMTA, DSC, and TGA, proved to be useful and adequate to characterize the degradation in soil process of a commercial biopolymer material (Mater-Bi class Y).

The various components of this polymeric blend, starch and cellulose derivatives, behaved differently during the soil burial test. On the one hand, the

starch region was strongly affected by the degradation process. The starch chains tended to progressively disappear from the polymeric structure from the beginning of the experiment and were totally removed after 87 days. In this sense, two distinct behaviors were observed in the starch region because amylose chains seemed to be removed easier than amylopectin chains. By contrast, the cellulose derivatives chains seemed to remain unaltered after 212 days of degradation in soil.

References

1. Bastioli, C. *Polym Degrad Stab* 1998, 59, 263.
2. Albersson, A.-C. *J Macromol Sci Pure Appl Chem* 1993, 30, 757.
3. Chandra, R.; Rutsgi, R. *Prog Polym Sci* 1998, 23, 1273.

4. Grassie, N. *Developments in Polymer Degradation*; Elsevier Applied Science: London, 1987.
5. Allen G.; Bevington, J. C. *Comprehensive Polymer Science: Polymer Characterization*; Pergamon: Oxford, England, 1989.
6. Turi, E. *Thermal Characterization of Polymeric Materials*; Academic: New York, 1987.
7. *Testing of Plastics. Influence of Fungi and Bacteri Visual Evaluation. Change in Mass and Physical Properties*; Deutsches Institute für Normung: Berlin, 1984.
8. Ishida, Y.; Tocino, M.; Takanagi, M. *J Appl Polym Sci* 1959, 1-2, 227.
9. Okumura, M.; Norimoto, M.; Shiraishi, N.; Aso, K. *Cell Chem Technol* 1967, 13, 571.
10. McCrum, N. G.; Read, B. E.; Williams, G. *Anelastic and Dielectric Effects in Polymeric Solids*; Dover: New York, 1991.
11. Riande, E.; Díaz-Calleja, R.; Prolongo, M. G. *Polymer Viscoelasticity: Stress and Strain in Practice*; Marcel Dekker: New York, 2000.
12. De Graaf, R. A.; Karman, A. P.; Janssen, L. P. B. M. *Starch/Stärke* 2003, 55, 80.
13. Avérous, L.; Fringant, C.; Moro, L. *Polymer* 2001, 42, 6565.
14. Aggarwal, P.; Dollimore, D. *Thermochim Acta* 1997, 291, 65.
15. Mano, J. F.; Koniarova, D.; Reis, R. L. *J Mater Sci Mater Med* 2003, 14, 127.
16. Sousa, F. S.; Barreto, A. P. G.; Macédo, R. O. *J Therm Anal Cal* 1998, 64, 739.
17. Kweon, D. K.; Cha, D. S.; Park, H. J.; Lim, S. T. *J Appl Polym Sci* 2000, 78, 986.
18. Blennow, A.; Bay-Smidt, A. M.; Olsen, C. E.; Moller, B. L. *Int J Biol Macromol* 2000, 27, 211.
19. Broido, A. *J Polym Sci Part A-2: Polym Phys* 1969, 7, 1761.